Angular momentum transfer torques in spin valves with perpendicular magnetization

Xingtao Jia, Ying Li, and Ke Xia
Department of Physics, Beijing Normal University, Beijing 100875, China

Gerrit E. W. Bauer
Kavli Institute of NanoScience, Delft University of Technology, NL-2628 CJ Delft, The Netherlands and Institute for Materials Research, Tohoku University, Sendai 980-8577, Japan

(Received 15 July 2011; revised manuscript received 31 August 2011; published 5 October 2011)

Spin valves incorporating perpendicularly magnetized materials are promising structures for memory elements and high-frequency generators. We report the angular dependence of the spin-transfer torque in spin valves with perpendicular equilibrium magnetization computed by first-principles circuit theory and compare results with experiments by Rippard *et al*. [Phys. Rev. B **81**, 014426 (2010)] on the CoFe|Cu|CoNi system. Furthermore, we predict a nonmonotonous (wavy) spin-transfer torque when the Cu spacer is replaced by a Ru layer.

DOI: 10.1103/PhysRevB.84.134403 PACS number(s): 72.25.Ba, 85.75.−d, 72.10.Bg

I. INTRODUCTION

A current can be used to read out the information in magnetic-memory devices by the giant magnetoresistance. Magnetic random access memory technology has become scalable by writing information using the current-induced spin-transfer torques (STTs).[1–4] The critical electric current density j_c necessary to switch a magnetic layer in a spin-valve structure is an all-important figure of merit in this case. The introduction of materials with perpendicular magnetocrystalline anisotropies that force the equilibrium magnetization out of the plane,[5] has helped to reduce j_c.[6–8]

Co|Ni multilayers are an interesting system with perpendicular anisotropy,[6,9,10] with a higher polarization and less spin-flip scattering than, for example, a CoPt alloy.[11] Rippard *et al*.[12] studied current-induced high-frequency generation in structures with a perpendicularly polarized $(\mathrm{Co|Ni})_n$ multilayer serving as the switchable magnet and an in-plane magnetized Co layer as a polarizer. The output power of such a device depends sensitively on the asymmetry of the angular-dependent STT when the magnetization of the free layer is reversed.[1,2,13] By generating an rf output by a dc current in a spin valve in which the free layer is magnetized normal to the polarizing layer, Rippard *et al*. parametrized the skewness of the torque as a function of the magnetization angle.[12] Koyama *et al*.[14] measured high-speed current-induced domain-wall velocities (40 m/s) in magnetic perpendicular Co|Ni multilayers with a current-in-plane configuration. Another interesting materials system is Co|Ru,[15,16] which also displays perpendicular magnetic anisotropy.[17]

Semiclassical theories[18,19] that combine a quantum treatment of the interface scattering and diffusion treatment of bulk scattering, in general, explain experiments on magnetic metallic multilayers well.[2] Here, we report calculations of the STTs of spin valves containing perpendicularly oriented ferromagnetic (F) materials based on magnetoelectronics circuit theory using interface transport parameters computed by first principles. The spin-orbit coupling is the origin of the magnetic crystalline anisotropy and perpendicular magnetization. However, the experimental spin-dependent interface resistances for not too heavy elements can be reproduced by parameter-free calculations without taking the spin-orbit interaction into account,[20] which will, therefore, be disregarded in the following.

Here, we study the angular-dependent STT in $\mathrm{Co_1Ni}_x$-based (the subscripts refer to the number of atomic layers) spin valves by circuit theory in combination with first-principles calculations. First, we present results for $\mathrm{Co|Cu|(Co_1Ni}_x)_y\mathrm{Co_1|Cu}(111)$ structures, where the subscripts 1 and x again indicate the number of atomic layers, while y is the number of stacks and compare them with experiments.[12] Next, we report large and wavy angular-dependent STTs for $\mathrm{Co|Ru|(Co_1Ni_2)}_x\mathrm{Co_1|Ru}(111)$ spin valves, which therefore, might be very efficient high-frequency generators.

In Sec. II, we introduce our method to calculate the STTs in spin valves in terms of the spin-mixing conductances of the interfaces computed from first principles, including corrections for the magnetically active bulk material and the diffusive environment. In Sec. III, we present results for the spin-mixing conductances for the two types of spin valves with perpendicular magnetic anisotropy and compute the angular dependence of STTs by magnetoelectronic circuit theory. We summarize our results in Sec. IV.

II. SPIN-MIXING CONDUCTANCE IN A DIFFUSIVE ENVIRONMENT

The STT due to a current bias I in F|normal-metal|F (F|N|F) spin valves in which the magnetizations are at an angle θ can be computed analytically by circuit theory[2,21] and, assuming structural symmetry, can be parametrized as[13]

$$\tau(\theta) = \frac{\hbar I \tilde{P}}{4e} \frac{\Lambda \sin\theta}{\Lambda \cos^2(\theta/2) + \Lambda^{-1}\sin^2(\theta/2)}, \qquad (1)$$

where the asymmetry parameter can be expressed in terms of the parameters of the N|F interface as $\Lambda = |\tilde{\eta}|/\sqrt{(1-\tilde{P}^2)\mathrm{Re}\,\tilde{\eta}}$, where $\tilde{\eta} = 2\tilde{G}_{\uparrow\downarrow}/(\tilde{G}_\uparrow + \tilde{G}_\downarrow)$ is the normalized effective spin-mixing conductance and $\tilde{P} = (\tilde{G}_\uparrow - \tilde{G}_\downarrow)/(\tilde{G}_\uparrow + \tilde{G}_\downarrow)$ is the conductance polarization. Here, $\tilde{G}_\uparrow$, $\tilde{G}_\downarrow$, and $\tilde{G}_{\uparrow\downarrow}$ are the spin-dependent and spin-mixing conductances, respectively, where the tilde indicates that they have been Schep corrected for a diffusive environment and

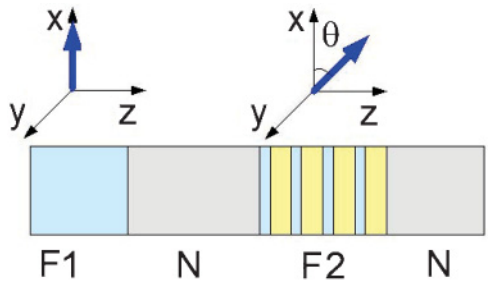

FIG. 1. (Color online) Scheme of asymmetric F1|N|F2|N spin valves with perpendicular magnetization F2 used in the calculations.

include the effects of the magnetically active contact regions close to the interface. In deriving Eq. (1), spin flip in the normal layer has been disregarded. When the spin-flip diffusion length in the magnetic layers is much longer than the bulk layer thickness,[2]

$$\frac{1}{\tilde{G}_\sigma} = \frac{1}{G_\sigma} + \frac{1}{2}\frac{e^2}{h}\left(\frac{\rho_{\mathrm{F},\sigma} d_\mathrm{F}}{A_\mathrm{F}}\right) - \frac{1}{2}\left(\frac{1}{G^{sh}_\mathrm{N}} + \frac{1}{G^{sh}_{\mathrm{F},\sigma}}\right), \qquad (2)$$

and

$$\frac{1}{\tilde{G}_{\uparrow\downarrow}} = \frac{1}{G_{\uparrow\downarrow}} - \frac{1}{2G^{sh}_\mathrm{N}}, \qquad (3)$$

where σ is the spin index, $d_{\mathrm{F(N)}}$ is the thickness of the F or the N layer, ρ is the bulk resistivity (for a single spin), and A_F is the pillar cross section. The G^{sh}'s are Sharvin conductances, $G_\uparrow = (e^2/h)\mathrm{tr}\,\mathbf{t}^\dagger_\uparrow\mathbf{t}_\uparrow$, $G_\downarrow = (e^2/h)\mathrm{tr}\,\mathbf{t}^\dagger_\downarrow\mathbf{t}_\downarrow$, and $G_{\uparrow\downarrow} = (e^2/h)\mathrm{tr}(\mathbf{I} - \mathbf{r}^\dagger_\uparrow\mathbf{r}_\downarrow)$, where $\mathbf{t}_{\downarrow(\uparrow)}$ ($\mathbf{r}_{\uparrow(\downarrow)}$) are the matrices of the transmission (reflection) coefficients of the phase-coherent region of the N|F contact as seen from the N and at the Fermi energy. $\mathbf{I}$ is an $M \times M$ unit matrix, where M is the number of conducting channels in N. The third term on the right-hand side of the last two equations is the Schep correction, while the second terms correct for the magnetically active bulk regions. When the F layer is much thicker than the spin-flip diffusion length l^F_{sd}, the latter should replace d_F in Eq. (2). With the spin-orbit interaction, we also ignore intrinsic spin-flip scattering at the interfaces. The F layers are assumed sufficiently thick such that the mixing transmission contribution may be disregarded.[22] Note that Eq. (1) only holds for structurally symmetric spin valves. In the following, we use the general expression in which the left and right interface parameters differ, as shown in Fig. 1 but do not list the expressions explicitly here (see Refs. 21,23–25).

In our calculations, the atomic potentials were determined in the framework of the tight-binding (TB) linear muffin-tin-orbital (MTO) method[26] based on density functional theory in the local-density approximation and an exchange-correlation potential parametrized by von Barth and Hedin.[27] The self-consistent crystal potentials were used as an input to a TB-MTO wave-function-matching calculation, from which we obtained the transmission and reflection at the interfaces. The calculations are carried out with a $\mathbf{k}_\parallel$ mesh density equivalent to more than 3600 $\mathbf{k}_\parallel$ mesh points in the two-dimensional Brillouin zone corresponding to the interface unit cell. The technical details can be found in Ref. 28. Table I compiles our results for various interface conductances including the bulk corrections due to magnetically active regions.

TABLE I. Parameters for clean (disordered) interfaces (in units of $10^{15}\ \Omega^{-1}\,\mathrm{m}^{-2}$). $X_n = (\mathrm{Co_1Ni_2})_n\mathrm{Co_1}$; $Y_n = (\mathrm{Co_1Ni_3})_n$; fcc Cu and Ru have Sharvin conductances of $G^{sh}_\mathrm{Cu} = 0.55 \times 10^{15}\ \Omega^{-1}\,\mathrm{m}^{-2}$ and $G^{sh}_{\mathrm{Ru(fcc)}} = 0.98 \times 10^{15}\ \Omega^{-1}\,\mathrm{m}^{-2}$, respectively. $G^{sh}_{\mathrm{Co(fcc)},\uparrow} = 0.47$ and $G^{sh}_{\mathrm{Co(fcc)},\downarrow} = 1.09 \times 10^{15}\ \Omega^{-1}\,\mathrm{m}^{-2}$ for majority and minority spins, respectively, in fcc Co. For hex Ru's, $G^{sh}_{\mathrm{Ru(hex)}} = 0.80 \times 10^{15}\ \Omega^{-1}\,\mathrm{m}^{-2}$ and Co with a hex Ru structure $G^{sh}_{\mathrm{Co(hex)},\uparrow} = 0.40$, and $G^{sh}_{\mathrm{Co(hex)},\downarrow} = 0.80 \times 10^{15}\ \Omega^{-1}\,\mathrm{m}^{-2}$ for majority and minority spins, respectively. A magnetically active bulk region correction is implemented for the normalized spin polarization $\tilde{P}$ and relative mixing conductance $\tilde{\eta}$. For the Cu|Co interface, we use $d_\mathrm{Co} = 5$ nm (Ref. 12) and bulk resistivity $\rho_\mathrm{Co} = 60\ \Omega\,\mathrm{nm}$ with spin asymmetry $\beta = 0.46$, which results in $\rho^\uparrow_\mathrm{Co} = 81\ \Omega\,\mathrm{nm}$ and $\rho^\downarrow_\mathrm{Co} = 219\ \Omega\,\mathrm{nm}$ (Ref. 31). We use a spin diffusion length of $l^\mathrm{Co}_{sd} = 60$ nm.

System	$G_\uparrow$	$G_\downarrow$	$\mathrm{Re}\,G_{\uparrow\downarrow}$	$\mathrm{Im}\,G_{\uparrow\downarrow}$	$\tilde{P}$	$\tilde{\eta}$
Cu|X_2|Cu	0.41(0.41)	0.35(0.19)	0.55(0.54)	−0.02(−0.03)	0.25(0.69)	0.85(1.1)
Cu|X_3|Cu	0.41(0.41)	0.32(0.18)	0.56(0.54)	−0.03(−0.03)	0.36(0.72)	0.96(1.1)
Cu|X_4|Cu	0.41(0.41)	0.31(0.16)	0.56(0.54)	−0.03(−0.03)	0.39(0.75)	0.98(1.2)
Cu|X_5|Cu	0.41(0.41)	0.30(0.15)	0.55(0.54)	−0.03(−0.03)	0.42(0.77)	0.97(1.2)
Cu|Y_2|Cu	0.39(0.40)	0.30(0.21)	0.40(0.54)	−0.02(−0.03)	0.34(0.62)	0.62(1.2)
Cu|Y_3|Cu	0.39(0.39)	0.26(0.19)	0.39(0.54)	−0.02(−0.03)	0.46(0.64)	0.66(1.3)
Cu|Y_4|Cu	0.39(0.39)	0.24(0.17)	0.40(0.54)	−0.01(−0.03)	0.52(0.69)	0.71(1.3)
Ru|Co	0.32(0.29)	0.58(0.53)	0.92(0.88)	0.001(0.02)	−0.15(−0.17)	8.9(8.7)
Ru|X_2|Ru	0.25(0.25)	0.36(0.31)	1.03(0.94)	−0.02(0.02)	−0.26(−0.15)	4.8(4.6)
Ru|X_3|Ru	0.25(0.25)	0.35(0.27)	1.03(0.94)	−0.02(0.02)	−0.24(−0.05)	4.9(5.1)
Ru|X_4|Ru	0.25(0.25)	0.33(0.23)	1.03(0.94)	−0.02(0.02)	−0.19(0.06)	5.2(5.7)
Ru|X_5|Ru	0.25(0.25)	0.31(0.22)	1.03(0.94)	−0.02(0.02)	−0.15(0.08)	5.5(5.8)
Ru|X_6|Ru	0.25(0.25)	0.32(0.20)	1.03(0.94)	−0.02(0.02)	−0.19(0.14)	5.2(6.2)
hex-Ru|Co	0.20(0.23)	0.53(0.32)	0.83(0.71)	−0.01(0.01)	−0.28(−0.19)	10(7.9)
Cu|Co[a]	0.42(0.42)	0.36(0.33)	0.41(0.55)	0.01(0.03)	0.51(0.54)	1.2(2.0)

[a]Reference 30.

III. Co_1Ni_2|Cu AND Co_1Ni_2|Ru MULTILAYERS

We first focus on the Co|Ni multilayers, which we treat as phase-coherent regions, i.e., we compute the scattering matrix of the entire multilayers, which is then treated in the circuit theory of conventional spin valves just like a single interface. We present the spin-dependent and mixing conductances of Cu|X_n|Cu with [$X_n = (Co_1Ni_2)_nCo_1$]. Here, the Cu leads on both sides are semi-infinite. X_n denotes n repetitions of the Co_1Ni_2 multilayer unit. As in the experiments,[12] a Co atomic layer is added for better contact with the Cu reservoirs. Since samples have been grown by sputtering, we take interface disorder into account, which, in general, is well modeled by a 2 monolayer 50%–50% interfacial alloy $(Co_1Ni_2)_n \rightarrow ([Co_{0.5}Ni_{0.5}]Ni[Co_{0.5}Ni_{0.5}])_n$.[2] Spin-flip scattering at the Co|Ni interface will suppress any benefits of an even larger number of Co|Ni interfaces.[20] Therefore, here, we present only calculations with $n \leqslant 5$. The computed dimensionless mixing conductance $\tilde{\eta}$ is also listed in the table.

In the fcc crystal structure, Co and Ni have nearly identical band structures for the majority spin, which results in very transparent Co|Ni interfaces. The majority spin conductance, therefore, stays nearly constant with increasing n. For minority spin electrons, the scattering at the Co|Ni interface is much stronger. Consequently, the minority spin conductance decreases rapidly with an increasing number of Co|Ni interfaces.

Figure 2 shows the angular-dependent STT exerted on the right-hand side of F1|Cu|$(Co_1Ni_2)_5Co_1$|Cu (F1 = Co,$Co_{90}Fe_{10}$) spin valves with intermixed interfaces calculated by our first-principles circuit theory and compared with the experimental result.[12] For pure Co as a fixed lead, we vary d_{Co} from 5 to 20 nm and find that the angular-dependent STT falls into the experimental range[12] estimated by Slonczewski's formula for symmetric spin valves with $\Lambda = 1.3$ and 1.7. Experimentally, $Co_{90}Fe_{10}$ is used as a fixed layer. Its spin-flip diffusion length is shorter than that of Co, but its resistivity is also higher, so there is not much difference when compared with a Co polarizer. We assume that the interface is not affected. We plot the results of CoFe in Fig. 2 with $d_{Co_{90}Fe_{10}} =$ 2.5 nm (Refs. 31 and 32), and $\rho_{Co_{90}Fe_{10}} = 154\ \Omega$ nm and is very similar to pure Co with $d_{Co} = 5$ nm. The results for Co|Cu|$(Co_1Ni_x)_yCo_1$|Cu from $x = 2$ to 3 and $y = 2$–5 are shown in Fig. 3. We observe large differences between epitaxial and disordered samples but only weak dependences on $x$and y. The results for epitaxial (disordered) samples fall into the range of Slonczewski's $\Lambda = 1.05$–1.15 (1.4–1.5).

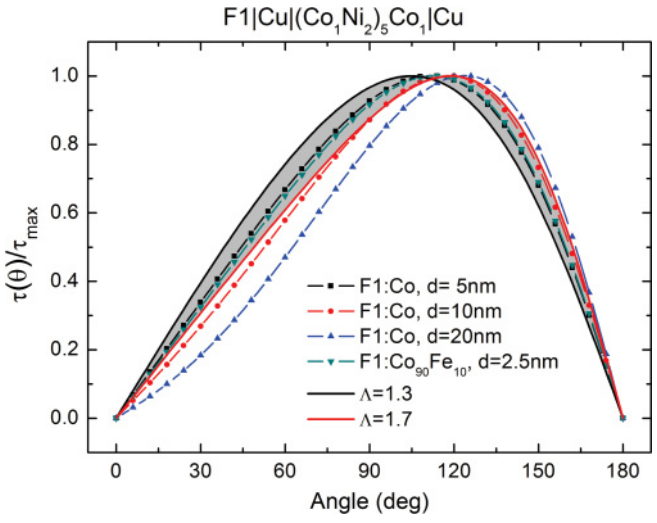

FIG. 2. (Color online) Comparison of computed and experimental (Ref. 12) angular-dependent STTs in F1|Cu|$(Co_1Ni_2)_5Co_1$|Cu (F1 = Co,$Co_{90}Fe_{10}$) spin valves with 2 monolayer 50%–50% intermixed interfaces. For Co as a fixed lead, we vary the thickness d_{Co} from 5 to 20 nm. When using $Co_{90}Fe_{10}$ as a fixed layer, we use $d_{Co_{90}Fe_{10}} = 2.5$ nm, resistivity $\rho_{Co_{90}Fe_{10}} = 154\ \Omega$ nm (Ref. 29), and Co|Cu interface parameters. The dark area indicates the experimental results parametrized by Slonczewski's formula with $\Lambda = 1.3$ and $\Lambda = 1.7$. Calculations are carried out by circuit theory for an asymmetric spin valve with first-principles interface parameters using the Schep correction including the contribution from the magnetically active region of the bulk F as described in the text.

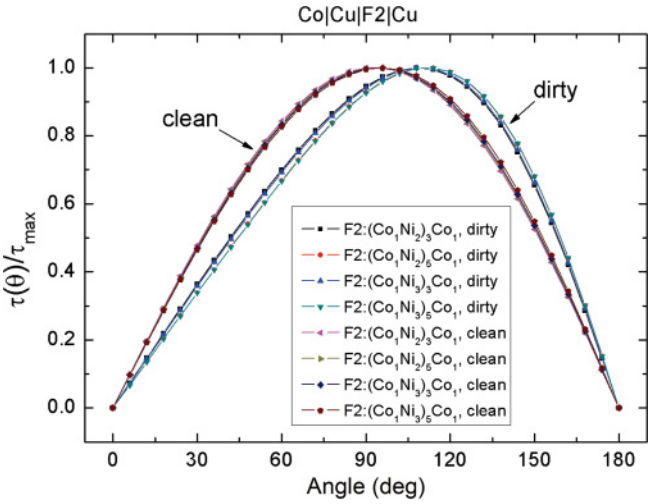

FIG. 3. (Color online) Angular-dependent STTs in Co|Cu |$(Co_1Ni_2)_xCo_1$|Cu and Co|Cu|$(Co_1Ni_3)_xCo_1$|Cu spin valves with $d_{Co} = 5$ nm.

The experimental results were parametrized by Eq. (1) for a structurally symmetric spin valve, whereas, our results were based on the theory for asymmetric structures.[21] We suggest that, in future experiments, Slonczewski's formula should be replaced by a more accurate parametrization.

Another interesting material with perpendicular magnetic anisotropy is Co|Ru. Experimentally, both hcp(0001) (Ref. 33) and fcc(111) (Ref. 34) structures have been reported. Despite the large lattice mismatch between Co and Ru, hcp Co|Ru could be grown epitaxially, and the magnetic anisotropy depends on the thickness of the Co layer.[35] However, the metastable structure relaxes to a more stable one after annealing.[35] Co|Ru|Co with a metastable fcc(111) structure has also been reported.[36] Here, we present systematic calculations of the transport properties of Co|Ru pillars with different structure and lattice constants as listed in Table II.

For epitaxial samples, we show results for an fcc(111) texture with lattice parameters for Ru, Co, and its average. The lattice parameter along the growth direction is varied to keep the atomic volume constant. Both spin polarization and

TABLE II. Comparison of the calculated spin polarization $\tilde{P}$ (we use $d_{\mathrm{Co}} = 5$ nm) and specific interface resistances $A\tilde{R} = A/\tilde{G}$ of clean (disordered) Co|Ru for different lattice parameters from the experiment.

System	Lattice	$\tilde{P}$	AR ($10^{-15}\ \Omega\,\mathrm{m}^2$)
fcc(111)	Ru	−0.12 (−0.05)	0.56 (0.83)
fcc(111)	Co	−0.14 (−0.20)	0.67 (0.93)
fcc(111)	(Ru + Co)/2	−0.09 (−0.02)	0.60 (0.87)
fcc(111)	Matching[a]	−0.15 (−0.17)	0.75 (0.86)
hcp(0001)	Ru[b]	−0.55 (−0.39)	0.78 (0.69)
hcp(0001)	Matching[a]	−0.28 (−0.19)	0.93 (0.98)
Experiment[34]		−0.2	0.5

[a]The 14 × 14 Co matched to 13 × 13 Ru.[33,37]
[b]Cobalt's atomic volume expanded to that of Ru.

specific resistance are close to the experimental values,[34] but considering the large lattice distortion (7.3%–14%), this may be accidental.

For the epitaxial hcp(0001) texture, our calculations yield very high spin polarizations $\tilde{P} = -39$ to -55% for both clean and dirty interfaces when Co adopts the Ru structure and lattice constants as reported[38] and small specific resistances $A\tilde{R} = A/\tilde{G} = 0.69$–$0.78 \times 10^{-15}\ \Omega\,\mathrm{m}^2$. Here and below, $\tilde{P}$ and $\tilde{G}$ have been Schep corrected with a magnetically active layer thickness $d_{\mathrm{Co}} = 5$ nm. Note that the structure is metastable, and under annealing, Co is expected to return to its normal lattice parameter.

To simulate sputtering conditions, a 14 × 14 Co is matched to a 13 × 13 Ru lateral supercell for both fcc(111) and hcp(0001), leading to a spin polarization of $\tilde{P} = -15\%$ and a specific resistance of $AR = 0.75 \times 10^{-15}\ \Omega\,\mathrm{m}^2$ for a clean fcc(111) texture, and $\tilde{P} = -28\%$ and $A\tilde{R} = 0.93 \times 10^{-15}\ \Omega\,\mathrm{m}^2$ for a clean hcp(0001) texture. A 50%–50% interface alloy has little effect on the fcc(111) texture but leads to a reduced $\tilde{P} = -19\%$ for the hcp(0001) texture. The measured spin polarization for the Co|Ru interface is $\tilde{P} = -20\%$ with specific resistance $A\tilde{R} = 0.5 \times 10^{-15}\ \Omega\,\mathrm{m}^2$ (Ref. 34).

In Table I, we observe that, in contrast to the Co|Cu interface, Co|Ru has a negative spin polarization for both fcc(111) and hcp(0001) orientations. Interesting is the relatively large dimensionless mixing conductance $\tilde{\eta}$. The predicted very large mixing conductance implies a large skewness of the angular-dependent STT, which makes this material promising for applications in high-frequency generators.

Figure 4 gives the angular dependent T/I in Co|Ru|FM|Ru(111) spin valves. Here, disorder is modeled again by 2 monolayers of a 50%–50% interface alloy (to rather small effect), and Schep and magnetic bulk corrections have been implemented. When fitted by Slonczewski's formula, the STT on the soft Co_1Ni_2 multilayer in the strongly asymmetric spin valve Co|Ru|$(Co_1Ni_2)_yCo_1$|Ru(111) shows a large variation in skewness in terms of the parameter $\Lambda = 0.5$–2.0. The maximum of the angular-dependent spin torque is shifted gradually from a low angle to a high angle when the thickness of Co_1Ni_2 increases from two to six periods. When Co serves as the free layer, the (modulus of the) angular-dependent torkance shows two peaks and a

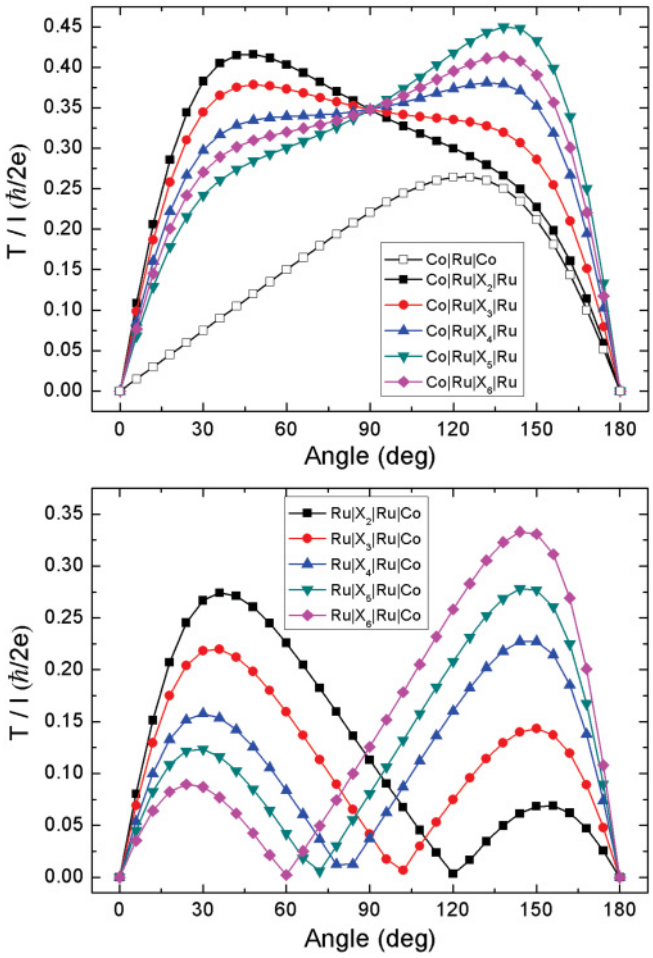

FIG. 4. (Color online) Angular-dependent torkance T/I on the right-side F in disordered Ru-based spin valves with $X_n = (Co_1Ni_2)_nCo_1$. The Co and Ru buffer layers are assumed to be much thicker than the spin-diffusion lengths l_{sd}^{Co} and l_{sd}^{Ru} so that the Schep correction includes the bulk scattering for the latter length scales (see Ref. 39). We disregard the bulk scattering in the Ru spacer, which should be allowed for the small thickness of 8 monolayers (2.21 nm) considered.

compensation point when the thickness of Co_1Ni_2 increases from three to five periods. This shape can be understood in terms of the spin accumulation in the N spacer in the parallel configuration,[40] which is accompanied by a nonmonotonic angular magnetoresistance. This behavior has been observed in Py|Cu|Co and has been dubbed wavy torques.[41,42]

IV. SUMMARY

We studied the angular-dependent STTs for materials with magnetization normal to the interfaces by circuit theory in combination with first-principles calculations. An interesting angular-dependent STT is found in the Co|Ru|$(Co_1Ni_2)_xCo_1$|Ru(111) spin valve. Moreover, a wavy angular-dependent STT acts on the Co layer in Co|Ru|$(Co_1Ni_2)_xCo_1$|Ru(111) structures. When CoNi is the free layer, we expect very efficient high-frequency generation.

ACKNOWLEDGMENTS

The authors acknowledge Y. Xu and S. Wang for their preliminary work. The authors gratefully acknowledge financial support from the National Basic Research Program of China (973 Program) under Grant No. 2011CB921803 and NSF-China Grant No. 60825404, the Dutch FOM Foundation, DFG Priority Program SpinCaT, and EU-ICT-7 Contract No. 257159 MACALO.

[1] J. Slonczewski, J. Magn. Magn. Mater. **159**, L1 (1996).
[2] A. Brataas, G. E. W. Bauer, and P. J. Kelly, Phys. Rep. **427**, 157 (2006).
[3] L. Berger, Phys. Rev. B **54**, 9353 (1996).
[4] E. B. Myers, D. C. Ralph, J. A. Katine, R. N. Louie, and R. A. Buhrman, Science **285**, 867 (1999).
[5] A. D. Kent, B. Ozyilmaz, and E. del Barco, Appl. Phys. Lett. **84**, 3897 (2004).
[6] S. Mangin, D. Ravelosona, J. A. Katine, M. J. Carey, B. D. Terris, and E. E. Fullerton, Nat. Mater. **5**, 210 (2006).
[7] S. Mangin, Y. Henry, D. Ravelosona, J. A. Katine, and E. E. Fullerton, Appl. Phys. Lett. **94**, 012502 (2009).
[8] H. Yoda *et al*., Curr. Appl. Phys. **10**, e87 (2010).
[9] G. H. O. Daalderop, P. J. Kelly, and F. J. A. den Broeder, Phys. Rev. Lett. **68**, 682 (1992).
[10] W. Chen, J. M. L. Beaujour, G. de Loubens, A. D. Kent, and J. Z. Sun, Appl. Phys. Lett. **92**, 012507 (2008).
[11] K. Inomata and Y. Saito, Appl. Phys. Lett. **73**, 1143 (1998).
[12] W. H. Rippard, A. M. Deac, M. R. Pufall, J. M. Shaw, M. W. Keller, S. E. Russek, G. E. W. Bauer, and C. Serpico, Phys. Rev. B **81**, 014426 (2010).
[13] J. Slonczewski, J. Magn. Magn. Mater. **247**, 324 (2002).
[14] T. Koyama, G. Yamada, H. Tanigawa, S. Kasai, N. Ohshima, S. Fukami, N. Ishiwata, Y. Nakatani, and T. Ono, Appl. Phys. Express **1**, 101303 (2008).
[15] S. S. P. Parkin, N. More, and K. P. Roche, Phys. Rev. Lett. **64**, 2304 (1990).
[16] C. Song, X. X. Wei, K. W. Geng, F. Zeng, and F. Pan, Phys. Rev. B **72**, 184412 (2005).
[17] J. Miyawaki, D. Matsumura, H. Abe, T. Ohtsuki, E. Sakai, K. Amemiya, and T. Ohta, Phys. Rev. B **80**, 020408(R) (2009).
[18] A. Brataas, Y. V. Nazarov, and G. E. W. Bauer, Phys. Rev. Lett. **84**, 2481 (2000); Eur. Phys. J. B **22**, 99 (2001).
[19] M. D. Stiles and A. Zangwill, Phys. Rev. B **66**, 014407 (2002).
[20] H. Y. T. Nguyen, R. Acharyya, E. Huey, B. Richard, R. Loloee, W. P. Pratt Jr., J. Bass, S. Wang, and K. Xia, Phys. Rev. B **82**, 220401(R) (2010).
[21] A. A. Kovalev, A. Brataas, and G. E. W. Bauer, Phys. Rev. B **66**, 224424 (2002).
[22] A. A. Kovalev, G. E. W. Bauer, and A. Brataas, Phys. Rev. B **73**, 054407 (2006).
[23] J. Xiao, A. Zangwill, and M. D. Stiles, Phys. Rev. B **70**, 172405 (2004).
[24] J. Barnas, A. Fert, M. Gmitra, I. Weymann, and V. K. Dugaev, Phys. Rev. B **72**, 024426 (2005).
[25] V. S. Rychkov, S. Borlenghi, H. Jaffres, A. Fert, and X. Waintal, Phys. Rev. Lett. **103**, 066602 (2009).
[26] I. Turek, V. Drchal, J. Kudrnovsky, M. Sob, and P. Weinberger, *Electronic Structure of Disordered Alloys, Surfaces and Interfaces* (Kluwer, Boston/London/Dordrecht, 1997).
[27] U. von Barth and L. Hedin, J. Phys. C **5**, 1629 (1972).
[28] K. Xia, M. Zwierzycki, M. Talanana, P. J. Kelly, and G. E. W. Bauer, Phys. Rev. B **73**, 064420 (2006).
[29] Y. Jiang, S. Abe, T. Nozaki, N. Tezuka, and K. Inomata, Phys. Rev. B **68**, 224426 (2003).
[30] K. Xia, P. J. Kelly, G. E. W. Bauer, A. Brataas, and I. Turek, Phys. Rev. B **65**, 220401(R) (2002).
[31] J. Bass and W. P. Pratt Jr., J. Magn. Magn. Mater. **200**, 274 (1999).
[32] K. Satoshi, A. Yasuo, M. Terunobu, and M. Shigemi, Jpn. J. Appl. Phys., Part 1 **45**, 3892 (2006).
[33] F. E. Gabaly, J. M. Puerta, C. Klein, A. Saa, A. K. Schmid, K. F. McCarty, J. I. Cerda, and J. de la Figuera, New J. Phys. **9**, 80 (2007).
[34] K. Eid, R. Fonck, M. A. Darwish, W. P. Pratt Jr., and J. Bass, J. Appl. Phys. **91**, 8102 (2002); C. Ahn, K.-H. Shin, and W. P. Pratt Jr., Appl. Phys. Lett. **92**, 102509 (2008).
[35] C. Liu and S. D. Bader, J. Magn. Magn. Mater. **119**, 81 (1993).
[36] P. J. H. Bloemen, H. W. van Kesteren, H. J. M. Swagten, and W. J. M. de Jonge, Phys. Rev. B. **50**, 13505 (1994).
[37] M. Grimsditch, J. E. Mattson, C. H. Sowers, S. D. Bader, and M. J. Peters, Phys. Rev. Lett. **77**, 2025 (1996).
[38] K. Rahmouni, A. Dinia, D. Stoeffler, K. Ounadjela, H. A. M. Van den Berg, and H. Rakoto, Phys. Rev. B. **59**, 9475 (1999).
[39] Y. Tserkovnyak, A. Brataas, and G. E. W. Bauer, Phys. Rev. B **66**, 224403 (2002).
[40] J. Manschot, A. Brataas, and G. E. W. Bauer, Phys. Rev. B **69**, 092407 (2004).
[41] O. Boulle, V. Cros, J. Grollier, L. G. Pereira, C. Deranlot, F. Petroff, G. Faini, J. Barnas, and A. Fert, Nat. Phys. **3**, 492 (2007).
[42] O. Boulle, V. Cros, J. Grollier, L. G. Pereira, C. Deranlot, F. Petroff, G. Faini, J. Barnas, and A. Fert, Phys. Rev. B **77**, 174403 (2008).